

# Low-profile, Broadband Polarization Converting Surface Ground Planes for Antenna Polarization Diversity

Brian A. Lail<sup>1</sup> and Kyu Y. Han<sup>2</sup>

<sup>1</sup> Department of Electrical and Computer Engineering  
Florida Institute of Technology, Melbourne, FL 32901, USA  
blail@fit.edu

<sup>2</sup> Wavebender, Inc.  
Milpitas, CA 95035  
ilrowa@hotmail.com

**Abstract**— A broadband antenna backed by a polarization converting surface ground plane is presented. The conversion of reflected field polarization provides diversity from a single, linearly polarized antenna, while avoiding broadside nulls in the radiation pattern as a function of frequency. Results for a low-profile dipole planar inverted cone antenna  $\sim\lambda/10$  above a polarization converting surface indicate greater than 40% bandwidth. Comparison with solid ground planes and high impedance ground planes are discussed, with polarization diversity and lack of broadside nulls identified as key advantages to the proposed design.

**Index Terms**— polarization converting surface, ground plane, polarization diversity, broadband antenna

## I. INTRODUCTION

Antennas are often placed above a ground plane to enhance the directivity in the topside half-plane. Antennas over a solid conducting ground plane require a  $\lambda/4$  standoff in order to produce constructive phase combinations for maximum directivity in the broadside direction. This result is due to radiation which propagates in the backside direction, reflects off the conducting plane with a  $\pi$  phase shift, and combines in-phase with the direct radiation in the broadside direction. By placing periodic conducting structures on a substrate over, but electrically close to, the solid conducting plane the reflection phase shift can be engineered. A high impedance ground plane, sometimes called an artificial magnetic conductor

(AMC), results when the reflection phase is zero, such that a standoff height to the antenna is not required in order to achieve in-phase broadside addition [1], [2]. The ground plane is made up of a solid conducting plane, a standoff layer, and an array of elements forming the periodic structure. When a high impedance ground plane is formed with symmetric elements peak broadside gain is achieved for an antenna placed near this ground plane. For both the symmetric-element AMC and the solid ground plane, the polarization sensitivity of the antenna is preserved in the process of back reflected radiation. In this paper we show that by using asymmetric elements a ground plane can be designed that provides polarization diversity. The asymmetric elements serve as polarization converting surface (PCS) such that a linearly polarized incident field is converted to its orthogonal polarization state upon reflection. Even though the antenna by itself is linearly polarized, the far-field combination of the direct field and the polarization-converted reflected field contains both polarization components. Furthermore, the PCS backed antenna does not suffer from nulls in the broadside radiation pattern as frequency is varied, as would be the case for a solid ground plane or AMC.

## II. POLARIZATION CONVERTING SURFACES

Twist reflectors have been used for nearly four decades in Cassegrain antenna systems to reduce aperture blocking [3]-[5]. For sake of discussion we will consider the asymmetric elements comprising the patterned surface as metallic strips.

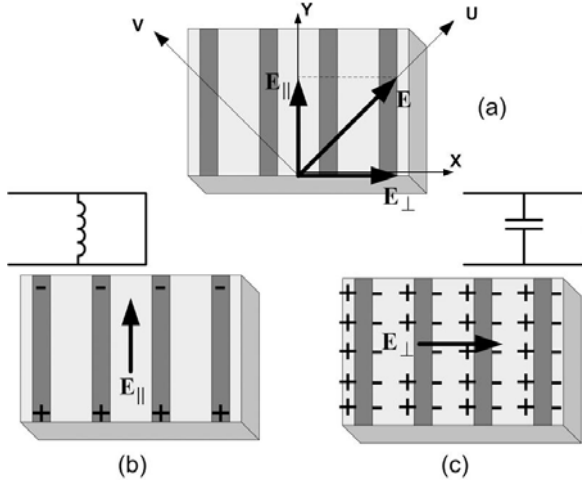


Fig. 1. Twist reflector basic mechanism. (a) The x-polarized E-field is resolved into two components: parallel and perpendicular to the metallic pattern. (b) and (c) charge distribution and their equivalent circuits.

The principle of operation of the twist reflector is understood by considering an incident plane wave with its electric field vector slanted at  $45^\circ$  with respect to the metallic strips. Then this electric field vector can be resolved into two equal components,  $E_{\parallel}$  and  $E_{\perp}$  as shown in Fig 1(a).

These components are in phase when the wave impinges onto the structure. Fig. 1(b) shows the parallel E-field component reflected through a structure equivalent to a shunt-inductive filter while Fig. 1(c) shows the perpendicular E-field component reflected through a shunt-capacitive filter [5]. As a result, the phase of the parallel component is advanced by the metallic strip while the perpendicular component is delayed. When the relative phase difference between two E-field components becomes  $180^\circ$ , the polarization vector is twisted by  $90^\circ$  upon reflection.

Polarization conversion has a unique signature depending on the observation coordinate system. In the XY configuration, as shown in Fig. 2, the co-polarized reflection phase is measured for the parallel and perpendicular orientation, and polarization conversion corresponds to a  $\pi$  relative phase between these components.

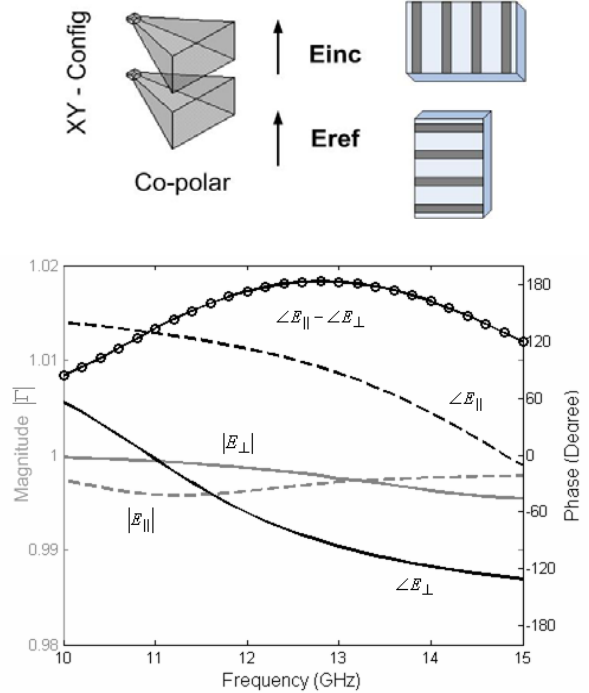


Fig. 2. Polarization conversion in the XY configuration occurs when the relative phase between x- and y-polarized reflected fields is approximately  $180^\circ$ .

In the UV orientation, polarization conversion occurs when the co-polarized reflection field magnitude is reduced while the cross-polarized reflection field magnitude is near unity, as shown in Fig. 3.

PCS have been designed using the genetic algorithm (GA) in order to achieve low-profile, broadband operation [6]. Fig. 4 is a characterization of polarization conversion through polarization loss, or the ratio of power in the converted polarization to the total reflected power.

$$Polarization\ Loss = PL = \frac{Desired\ Reflected\ Power}{Total\ Reflected\ Power}$$

A polarization loss greater than -0.1 dB corresponds to 98% power conversion. In Fig. 2 greater than 98% power in the incident linear polarization state is converted to the orthogonal polarization state over frequencies 9.5 – 11.7 GHz.

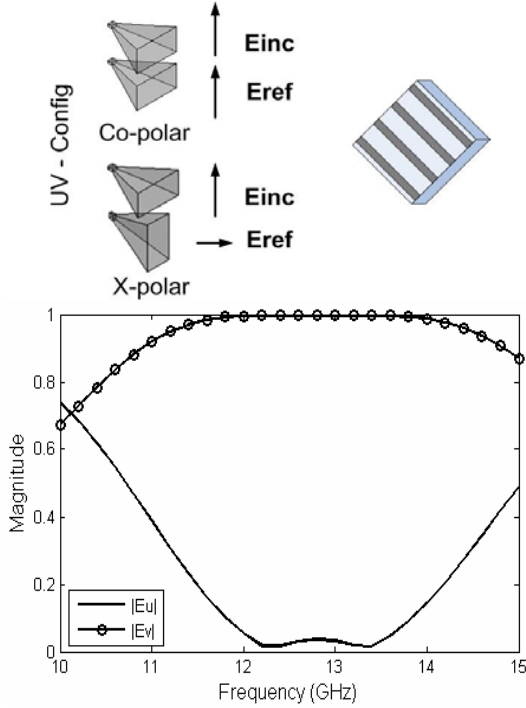


Fig. 3. In the UV coordinate system near unity magnitude of the cross-polarized reflected field represents polarization conversion.

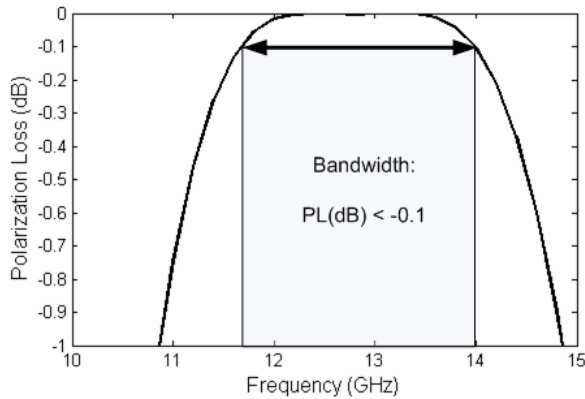


Fig. 4. Polarization Loss for the cases shown in Figures 2 and 3.

### III. GENETIC ALGORITHM

Fig. 5 shows an overall GA flow diagram that is employed to design a twist reflector. A chromosome is the binary form of a structure that includes all the parameter information.

Decoded chromosomes using binary-decoding method [7] are evaluated by HFSS. Once fitness values for all the members of a population are assigned, randomly selected members based on fitness values are evolved through reproduction process: crossover and mutation [8].

Among various strategies for selection and crossover, tournament selection and single-point crossover are employed in our implementation, respectively.

The common twist reflector with thickness  $0.25\lambda_0$  to  $0.358\lambda_0$  shows bandwidth of 10 – 25 % [9]-[12]. Some twist reflector models exhibit bandwidth of more than several octaves [5], [9] but these structures are constructed using multi-layers with thickness bigger than  $0.358\lambda_0$ . The purpose of this study is to generate a novel unit cell that exhibits a polarization converting property over a wide frequency range while keeping the thickness less than quarter-wavelength.

The goal of the GA in twist reflector design is to produce a relative phase difference of  $180^\circ$  between parallel and perpendicular response, as explained in the previous section. Equivalently, polarization conversion can be directly observed by co-polar and cross-polar magnitude responses. For example, for an x-polarized incident wave propagating in the z-direction, the fitness function can be described as:

$$\text{fitness function} = \max \left( \sum_{\text{freq}=8-14\text{GHz}} (|E_y| - (1 - |E_x|)) \right)$$

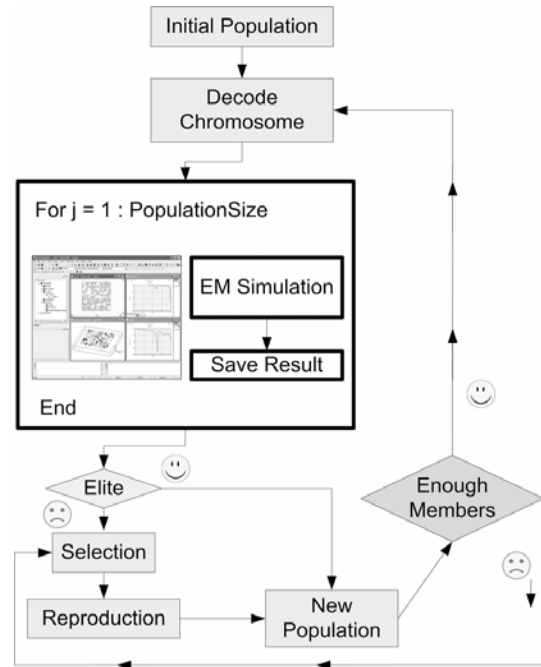


Fig. 5. Overall GA flow diagram.

#### IV. PCS DESIGNS

For unit cell design, there are a number of ways to parameterize the surface pattern. One popular way in the design of metamaterials is to form a unit cell with binary pixels where pixels with “0”s and “1”s represent empty spaces and conductors, respectively. In this way, GA can explore various surface shapes to generate an optimal solution. As an initial exercise of the GA tool a unit cell consisting of 16x16 binary pixels was the basis of a PCS design with fitness function targeting polarization conversion at  $9.5 \pm 0.3$  GHz. In order to avoid corner point contacts pixels were overlapped by 0.1 mm [14], [15].

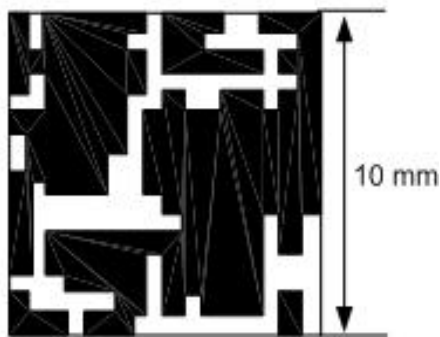


Fig. 6. Unit cell consisting of 16x16 binary pixels.

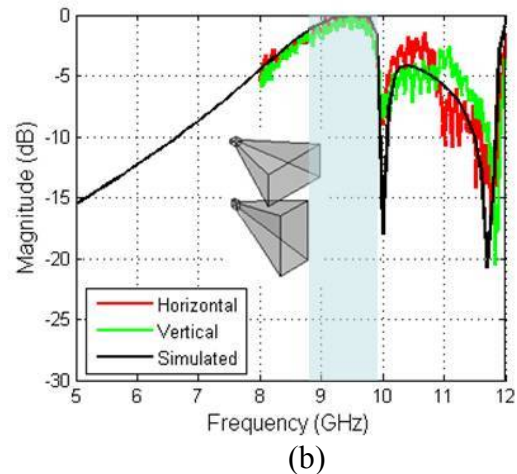
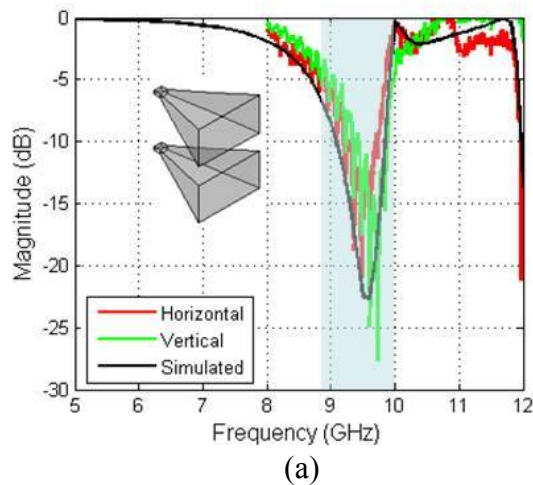
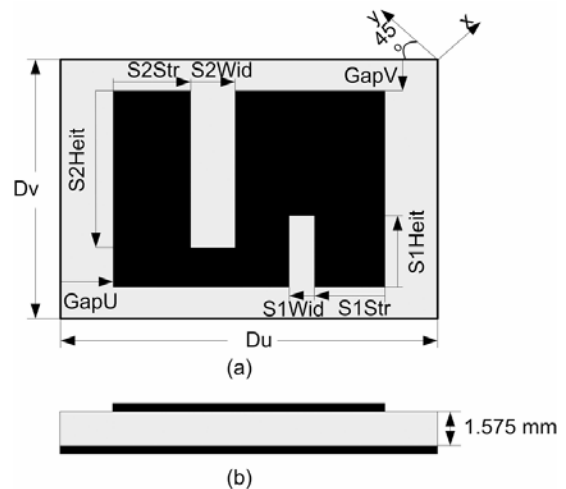
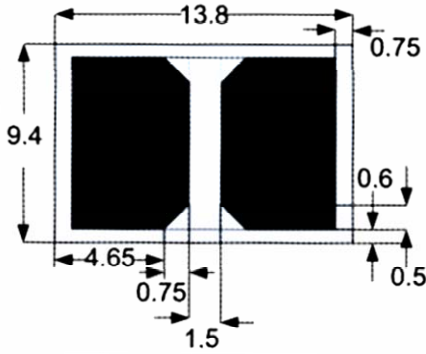


Fig. 7. Co-pol (a) and cross-pol (b) response of the initial GA designed PCS showing polarization conversion for  $9.5 \pm 0.3$  GHz. Simulated data is from Ansoft HFSS models.

A 21 cm x 14 cm PCS with the unit cell shown in Fig. 6 was fabricated on Duroid 5880 of thickness 1.575 mm. Measured and modeled results are shown in Fig. 7. While the pixelated unit cell design meets the fitness requirement for polarization conversion for  $f=9.5 \pm 0.3$  GHz, the performance falls off rapidly outside of this range of frequencies. Recognizing that the unit cell of Fig. 6(a) resembles a meandered structure, the parameter space was further constrained.



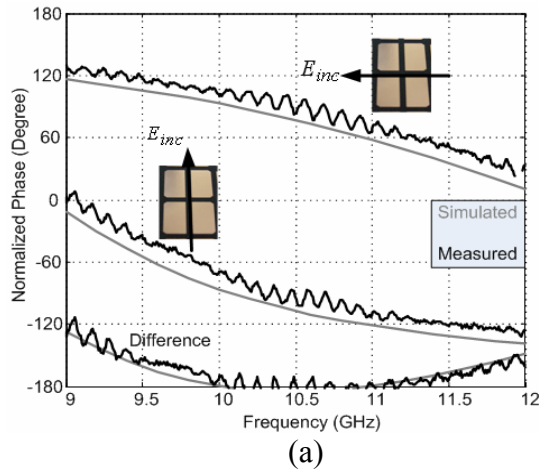


(c)

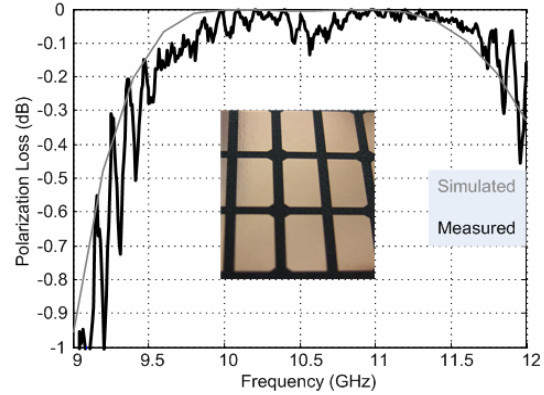
Fig. 8. GA parameter setup: top view (a), side view (b), and the optimized unit cell design (c).

The parameter space used to represent a unit cell in the optimized design is shown in Fig. 8. Based on twist reflector mechanism, the initial structure is rotated by  $45^\circ$  relative to the incident wave. Then, a rectangular conductor is generated inside of the unit cell and subtracted by two independent slots. In this way, GA can explore any size of rectangles, strip lines, and meanderline.

Ten parameters are involved in the GA process are shown in Fig. 8(a): unit cell width ( $D_u$ ) and height ( $D_v$ ), vertical ( $GapV$ ) and horizontal ( $GapU$ ) gap between the adjacent unit cells, and starting point ( $S1Str$  and  $S2Str$ ), width ( $S1Wid$  and  $S2Wid$ ), and height ( $S1Heit$  and  $S2Heit$ ) for two slots.



(a)



(b)

Fig. 9. PCS reflection phase (a) and polarization loss (b). Simulated data is from Ansoft HFSS models.

Fig. 8(c) shows the PCS unit cell geometry, while Fig. 9a shows modeled and measured reflection phase of the x- and y-components and the difference between these phases. Polarization is converted upon reflection when the difference in phase between the x- and y-components is  $\pi$  radians. Fig. 9b is a characterization of polarization conversion through polarization loss, or the ratio of power in the converted polarization to the total reflected power. A polarization loss greater than  $-0.1$  dB corresponds to 98% power conversion. Greater than 98% power in the incident linear polarization state is converted to the orthogonal polarization state over frequencies 9.5 – 11.7 GHz.

## V. PCS GROUNDPLANE BACKED ANTENNA

A linearly polarized antenna over a reflective ground plane is considered. For comparison, we include solid perfect conductor (PEC), AMC, and PCS ground planes in this discussion. For this treatment we assume perfect reflection and no losses. Consider a dipole antenna that is aligned with the uv-coordinate axes and the ground plane beneath the antenna contains elements that are periodic in and aligned with the xy-axes.

Using the total far-field expressions, the broadside gain for each case is plotted in Fig. 10. Since the PEC plane provides a  $\pi$  phase shift upon reflection we plot broadside gain as a function of standoff height  $d$ . For both AMC and PCS we consider a negligible standoff height and plot gain as a function of reflection phase shift.

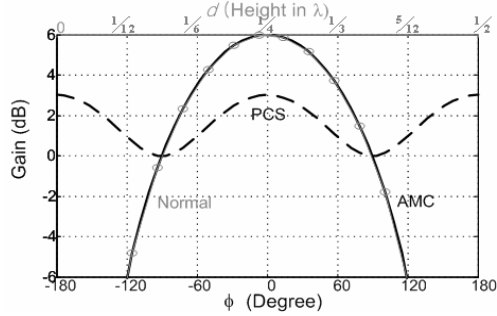


Fig. 10. Broadside power comparisons.

From Fig. 10 we see that while the PCS ground plane does not provide the peak broadside power of the PEC or AMC ground plane, the direct and reflected fields never add destructively so that there is never a broadside null. The PEC or AMC ground planes constrain broadband operation due to the nulls that develop in the total far field as wavelength moves away from the design value. Furthermore, the PCS and AMC fields are linearly polarized according to the alignment of the antenna.

Antenna elements with broadband performance are required to utilize with the proposed broadband PCS. One of the simplest structures that exhibit such a broadband performance is the Low-profile Dipole Planar Inverted Cone Antenna (LPdiPICA) [16], [17]. Fig. 11 shows the geometry and dimensions of the LPdiPICA antenna used in this work.

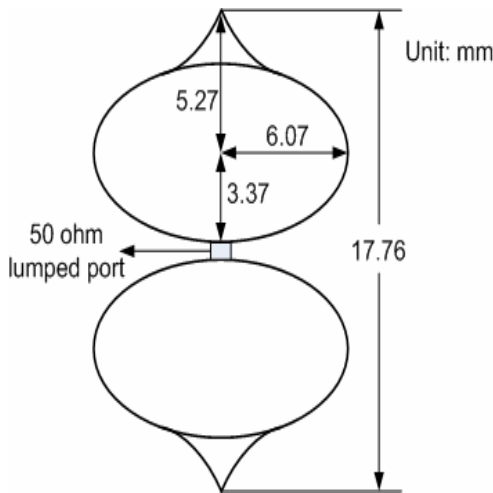


Fig. 11. LPdiPICA antenna.

The broadside gain of the LPdiPICA antenna shown in Fig. 11 is compared for three cases in Fig. 12. The black dashed line is the antenna with no back reflector. The blue curve is gain when the antenna is  $\lambda/4$  above a solid ground plane. The red curve is the LPdiPICA 3mm above a PCS ground plane. The solid ground provides maximum broadside gain, but as frequency is varied this gain falls off. LPdiPICA antenna above a PCS structure exhibits 5.7–7.1 dB gain over frequency range of 7–11 GHz, while providing diversity through the conversion of the reflected field polarization, and low-profile with a standoff height  $\sim\lambda/10$ .

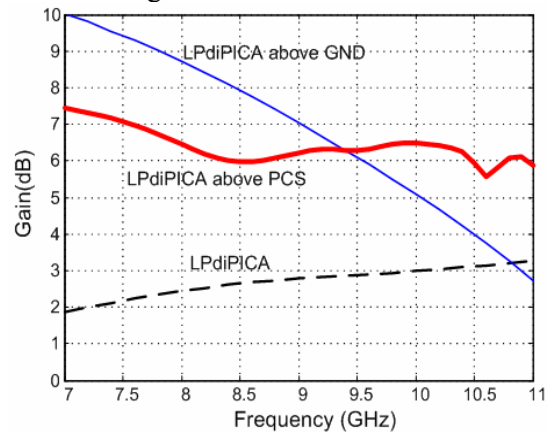


Fig. 12. LPdiPICA broadside gain.

## VI. CONCLUSIONS

The benefits of a PCS ground plane have been identified to be polarization diversity from a single, linearly polarized antenna and no nulls in the broadside radiation pattern as frequency is swept. The PCS achieves low profile geometry, much like AMC. However, by converting the reflected field polarization the far field combination of direct and reflected fields never destructively interfere, such that there are never nulls in the broadside radiation pattern. The trade-off is that the PCS ground plane does not have the peak broadside gain of a solid ground plane or AMC. A LPdiPICA antenna backed by a PCS ground plane was presented with greater than 40% bandwidth in the integrated design. When combined with a broadband antenna, the low-profile PCS ground plane provides both broadband operation and polarization diversity.

## REFERENCES

- [1] D. Sievenpiper, L. Zhang, R. F. J. Broas, N. G. Alexopolous, and E. Yablonovitch, "High-impedance electromagnetic surfaces with a forbidden frequency band," *IEEE Trans. Microwave Theory Tech.*, vol. 47, pp. 2059-2074, Nov. 1999.
- [2] A. P. Feresidis, G. Goussetis, S. Wang, and J. C. Vardaxoglou, "Artificial Magnetic Conductor Surfaces and Their Application to Low-Profile High-Gain Planar Antennas," *IEEE Trans. Antennas Propagat.*, vol. 53, no. 1, pp. 209–215, Jan. 2005.
- [3] P. W. Hannan, "Microwave Antennas Derived from the Cassegrain Telescope," *IRE Trans. Antennas Propagat.* Vol. 9, pp 140–153, Mar. 1961.
- [4] M. I. Skolnik, *Introduction to Radar Systems*, 3rd ed. New York: McGraw-Hill, 2001, pp. 661–672.
- [5] E. Orleansky, C. Samson, and M. Havkin, "A Broadband Meanderline Twistreflector for the Inverse Cassegrain Antenna." *Microwave J.*, vol. 30 no. 10, pp. 185 – 192, Oct. 1987.
- [6] K. Y. Han and B.A. Lail, "Genetically Engineered Meanderline Twist Reflector," IEEE Antennas and Propagation Society International Symposium, pp. 1-4, 5-11 July 2008.
- [7] J. M. Johnson and Y. Rahmat-Samii, "Genetic Algorithms in Engineering Electromagnetics," *IEEE Antennas Propagat. Mag.*, vol. 39, no. 4, pp. 7–21, Aug. 1997.
- [8] R. L. Haupt, "An Introduction to Genetic Algorithms for Electromagnetics," *IEEE Antennas and Propagation Magazine*, vol. 37, no. 2, pp. 7–15, April 1995.
- [9] H. Jasik, Ed., *Antenna Engineering Handbook* New York: McGraw-Hill, 1961, pp. 25– 6.
- [10] E. L. Holzman, "Transreflector Antenna Design for Millimeter-Wave Wireless Links," *IEEE Antennas and Propagat Mag.*, vol. 47, no. 5, pp. 9–22, Oct. 2005.
- [11] T., K. Wu, R. Palos, and D. L. Helms, "Meanderline Polarization Twister," U.S. Patent 4 786 914,, Nov. 22, 1988.
- [12] W. H. Shi, W. X. Zhang, and M. G. Zhao, "Novel Frequency-Selective Twist Polariser," *Electronics Lett.* 7th vol. 27, no. 23, pp. 2110–2111, Nov. 1991.
- [13] E. K. English and E. C. Saladin, "Electromagnetic-Field Polarization Twister," U.S. Patent 0 227 417, Dec. 11, 2003.
- [14] M. Ohira, H. Deguchi, M. Tsuji, and H. Shigesawa, "Multiband Single-Layer Frequency Selective Surface Designed by Combination of Genetic Algorithm and Geometry-Refinement Technique," *IEEE Trans. Antennas Propagat.*, vol. 52, no. 11, pp. 2925-2931, Nov. 2004.
- [15] M. John and M. J. Ammann, "Wideband Printed Monopole Design using a Genetic Algorithm," *IEEE Antennas Wireless Propagat. Lett.*, vol. 6, pp. 447–449, 2007.
- [16] S. Y. Suh, W. L. Stutzman, W. Davis, A. Waltho, and J. Schiffer, "A Novel Broadband Antenna, the Low-Profile Dipole Planar Inverted Cone Antenna (LPdiPICA)," IEEE Antennas and Propagation Society International Symposium, vol. 1, pp. 20–25, June 2004.
- [17] S. Y. Suh, A. E. Waltho, V. K. Nair, W. L. Stutzman, and W. A. Davis, "Evolution of Broadband Antennas from Monopole Disc to Dual-polarized Antenna," IEEE Antennas and Propagation. Society International Symposium, pp. 1631–1634, July 2006.